Babelyuk Valeriy, Gozhenko Anatoliy, Dubkova Galyna, Zukow Walery, Hubyts'kyi Viktor, Ruzhylo Sofiya, Fedyayeva Svitlana, Kovalchuk Galyna, Popovych Igor. Causal relationships between the parameters of gas discharge visualization and immunity. Pedagogy and Psychology of Sport. 2021;7(1):115-134. elSSN 2450-6605. DOI http://dx.doi.org/10.12775/PPS.2021.07.01.008
https://apcz.umk.pl/czasopisma/index.php/PPS/article/view/PPS.2021.07.01.008
https://zenodo.org/record/4603448

The journal has had 5 points in Ministry of Science and Higher Education parametric evaluation. § 8. 2) and § 12. 1. 2) 22.02.2019.

Received: 17.02.2021. Revised: 17.02.2021. Accepted: 04.03.2021.

CAUSAL RELATIONSHIPS BETWEEN THE PARAMETERS OF GAS DISCHARGE VISUALIZATION AND IMMUNITY

Valeriy Y. Babelyuk[1,2], Anatoliy I. Gozhenko[1], Galyna I. Dubkova[2], Walery Zukow[3], Viktor Y. Hubyts'kyi[2], Sofiya V. Ruzhylo[4], Svitlana I. Fedyayeva[5], Galyna Y. Kovalchuk[4], Igor L. Popovych[1,6]

[1]State Enterprise Ukrainian Research Institute for Medicine of Transport, Ministry of Health, Odesa, Ukraine prof.gozhenko@gmail.com
[2]Clinical Sanatorium „Moldova", Truskavets', Ukraine san.moldova.tr@ukr.net
[3]Nicolaus Copernicus University, Torun, Poland w.zukow@wp.pl
[4]Ivan Franko Pedagogical University, Drohobych, Ukraine doctor-0701@ukr.net
[5]Danylo Halyts'kyĭ National Medical University, L'viv, Ukraine svfedyaeva@ukr.net
[6]OO Bohomolets' Institute of Physiology NAS, Kyïv, Ukraine i.popovych@biph.kiev.ua

Background. Earlier, we found a close canonical correlation between parameters of gas discharge visualization (GDV) and principal neuroendocrine factors of adaptation. The **purpose** of this study is to elucidate the relationship between GDV and immunity parameters. **Material and research methods**. We observed twice 10 women and 10 men aged 33-76 years without clinical diagnose. In the morning in basal conditions at first registered kirlianogram by the method of GDV by the device "GDV Chamber" ("Biotechprogress", SPb, RF). For further analysis the following parameters were selected: Area, Shape Coefficient as ratio Square Length of outward contour gas discharge image to its Area as well as Entropy of contour in Right, Frontal and Left projections registered both with and without polyethylene filter. Estimated also Energy and Asymmetry of virtual Chakras. Then registered routine parameters of cellular and humoral Immunity. Results processed by method of canonical analysis, using the software package "Statistica 5.5". **Results.** According to the value of the canonical correlation coefficient R with GDV parameters, the immunity parameters are arranged in the following order: IgA (0,716; p=0,005), $CD8^+CD3^+$ Tc-lymphocytes (0,646; p=0,004), IgG (0,645; p=0,002), IgM (0,622; p=0,0001), "active" T-lymphocytes (0,572; p=0,007), $CD4^+CD3^+$ Th-lymphocytes (0,566; p=0,003), CIC (0,491; p=0,018), 0-lymphocytes (0,457; p=0,036), $CD16^+$ NK-lymphocytes (0,396; p=0,043), $CD22^+$ B-lymphocytes (0,439; p=0,105). The integral canonical correlation between the parameters of GDV and Immunity was very strong (R=0,994; $p<10^{-4}$). **Conclusion.** Between parameters of

Immunity and parameters of GDV exist strong canonical correlation suggesting relevance and informativenes this method.
Key words: Gas Discharge Visualization, Cellular and Humoral Immunity, Relationships.

INTRODUCTION

In 1996 KG Korotkov created a new scientific approach, based on the digital videotechnics, modern electronics and computer processing quantitative data, called as method gas discharge visualization (GDV bioelectrography). Parallel uses the terms kirlianography and electrophotonics [12,13]. Despite the initial obstruction of some conservative Western scientists, the GDV method is now considered quite relevant [8,14,21]. We are pleased to note that we are also a little involved in this recognition. In 2010 we launched a study on its verification. First, we found relationships between parameters GDV and HRV as well as blood pressure at 8 volunteers [23]. In the next study [1,25] we shown by means of 20 observations of 10 practically healthy men that between the eight basic parameters of GDV, on the one hand, and serum levels of triiodothyronine, testosterone and cortisol as well as mineralocorticoid activity, on the other hand, exist closely canonical correlation (R=0,947). A large contingent of 10 men and 10 women and broadened research methods confirmed the findings. Coefficient of canonical correlation parameters of GDV with Testosterone makes 0,81, with Cortisol 0,66, with Calcitonin 0,61, with Triiodothyronine 0,60, with Aldosterone 0,48. Among parameters HRV closely correlated with GDV constellation Bayevskiy's Stress Index (R=0,80) and LF/HF Ratio (R=0,76). Coefficient of canonical correlation between Neuroendocrine constellation, on the one hand, and parameters of GDV, on the other hand, makes 0,970 [2,4]. The same contingent shows that entropy of GDV correlates with the entropies of EEG, immunocytogram and leukocytogram but not HRV [6].

In addition, the response of GDV parameters to the course of use of bioactive water Naftussya [10], electrostimulation by device "VEB" [7,11], the course of rehabilitation by VI Kozyavkin's method [5,24,15,16], as well as the immediate response to Katas of Kyokushin Karate operator [3] were demonstrated.

The **purpose** of this study is to elucidate the relationship between GDV and immunity parameters.

MATERIAL AND RESEARCH METHODS

The object of observation were members of the same contingent: 10 women and 10 men aged 33-76 years without clinical diagnose but with dysfunction of neuro-endocrine-immune complex and metabolism, characteristic for premorbid (intermediate between health and illness) state.

In the morning on an empty stomach we registered kirlianogram by the method of GDV by the device of "GDV Chamber" ("Biotechprogress", SPb, RF). The first base parameter of GDV is **Area** of gas discharge image (GDI) in Right, Frontal and Left projections registered both with and without polyethylene filter. The second base parameter is a **Shape coefficient** (ratio of square of length of external contour of GDI toward his area), which characterizes the measure of serration/fractality of external contour. The third base parameter of GDI is **Entropy**, id est measure of chaos. Program estimates also **Energy** and **Asymmetry** of virtual **Chakras** [12-14].

Immune status evaluated on a set of I and II levels recommended by the WHO as described in handbook [17]. For phenotyping subpopulations of lymphocytes used the methods of rosette formation with sheep erythrocytes on which adsorbed monoclonal antibodies against receptors CD3, CD4, CD8, CD22 and CD16 from company "Granum"

(Kharkiv) with visualization under light microscope with immersion system. We carried out also test of “active” rosette formation. The state of humoral immunity judged by the concentration in serum of immunoglobulins classes G, A, M (ELISA, analyser “Immunochem”, USA) and circulating immune complicis (with polyethylene glycol precipitation method).

We calculated also the Entropy (h) of Immunocytogram (relative contents subpopulations of lymphocytes) using IL Popovych's [22,26] formula, which is based on CE Shannon's [29] formula:

$$h = -[CD4 \bullet \log_2 CD4 + CD8 \bullet \log_2 CD8 + CD22 \bullet \log_2 CD22 + CD16 \bullet \log_2 CD16]/\log_2 4$$

Every day four people were tested. A week later, all the tests were repeated. Results processed using the software package "Statistica 5.5".

RESULTS AND DISCUSSION

Educated in the spirit of Western medicine, we decided to look at the results through the eyes of adherents of Eastern medicine, ie the parameters of GDV were considered as an argument (cause), and the parameters of Immunity as a function (consequence). The association with geocentric and heliocentric concepts in astronomy, which equally served seafarers for orientation, comes to mind.

According to the formula:

$$|r| \geq \{exp[2t/(n-1,5)^{0,5}] - 1\}/\{exp[2t/(n-1,5)^{0,5}] + 1\},$$

for a sample of 40 observations critical value of correlation coefficient module at $p<0,05$ ($t>2,02$) is 0,31, at $p<0,01$ ($t>2,70$) is 0,41, at $p<0,001$ ($t>3,55$) is 0,52.

Among the parameters of cellular immunity, the relative level of T-killers in the blood correlates most closely with the parameters of GDV, in particular with Entropy of GDI in Left projection (Fig. 1).

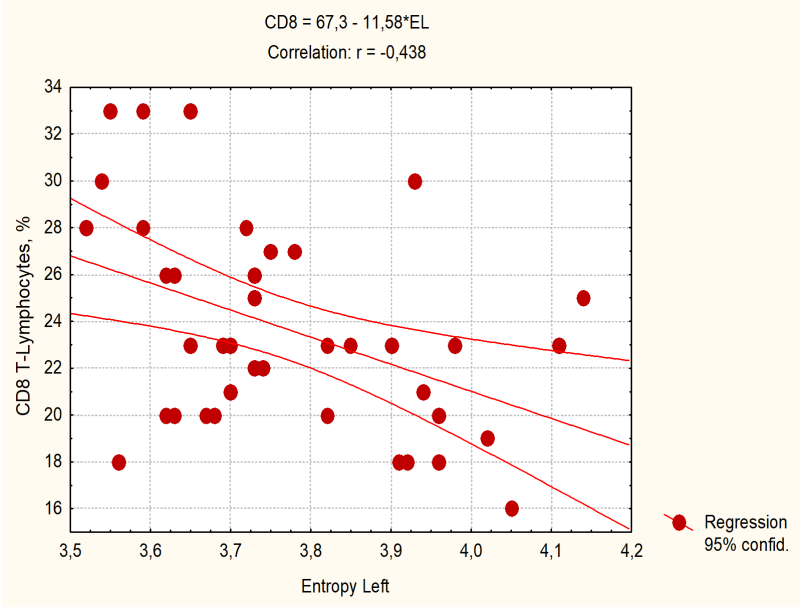

Fig. 1. Scatterplot of correlation between Entropy of GDI in Left projection (X-line) and $CD8^+CD3^+$ T-lymphocytes level (Y-line)

By stepwise exclusion to reach the maximum value of adjusted R^2, the regression model included six GDV parameters, the total impact of which on the level of T-killers is estimated at 31% (Table 1 and Fig. 2).

Table 1. Regression Summary for Dependent Variable: $CD8^+CD3^+$ Tc-lymphocytes
R=0,646; R^2=0,418; Adjusted R^2=0,312; $F_{(6,3)}$=3,9; $\chi^2_{(6)}$=18,9; p=0,004; SE: 3,6 %

		Beta	St. Err. of Beta	B	St. Err. of B	$t_{(33)}$	p-lev-el
	r		Intercpt	-15,52	63,03	-,25	,81
EL	-0,44	-,265	,148	-7,01	3,92	-1,79	,08
EL f	-0,37	-,146	,157	-3,59	3,86	-,93	,36
Ch5 E	-0,33	-,126	,143	-1,83	2,08	-,88	,39
Ch4 A	-0,30	-,199	,148	-2,73	2,03	-1,35	,19
Sym f	0,38	,202	,149	,84	,62	1,36	,18
Ch1 A f	0,36	,195	,153	4,59	3,59	1,28	,21

Abbreviations of GDV parameters: A – Area (pixels), E - Entropy, Sym – Symmetry (%), S – Shape coefficient, R – Right projection, F – Frontal projection, L – Left projection, f – with filter, ChE - Chakra Energy [E=(R+L)/2], ChA – Chakra Asymmetry (A=R-L).

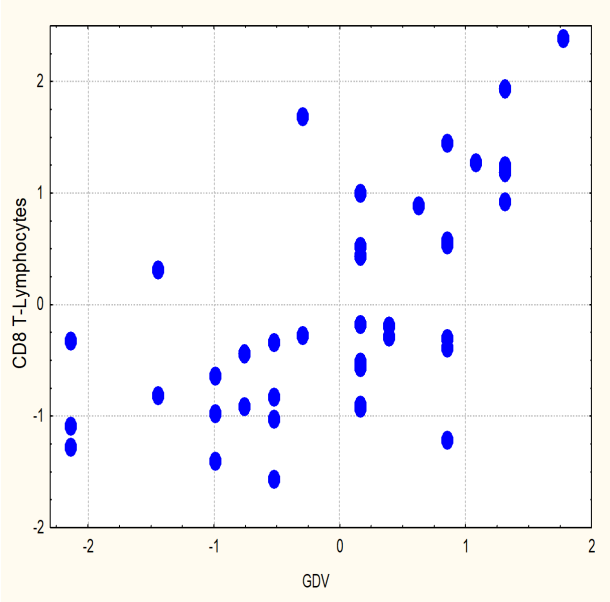

Fig. 2. Scatterplot of canonical correlation between GDV parameters (X-line) and $CD8^+CD3^+$ Tc-lymphocytes level (Y-line)

The level of T-helpers is upregulated by the symmetry of the GDI registered with the filter and the asymmetry of the seventh chakra, while it is negatively regulated by the energy of the sixth chakra. The degree of determination is 26% (Table 2 and Fig. 3).

Table 2. Regression Summary for Dependent Variable: $CD4^+$ $CD3^+$Th-lymphocytes
R=0,566; R^2=0,320; Adjusted R^2=0,264; $F_{(3,4)}$=5,7; $\chi^2_{(3)}$=14,1; p=0,003; SE: 4,4 %

		Beta	St. Err. of Beta	B	St. Err. of B	$t_{(36)}$	p-level
	r		Intercpt	-127,1	63,6	-2,00	,053
Sym f	0,35	,361	,140	1,75	,68	2,57	,014
Ch7 A f	0,30	,351	,139	8,42	3,32	2,53	,016
Ch6 E f	-0,32	-,265	,139	-5,16	2,71	-1,91	,065

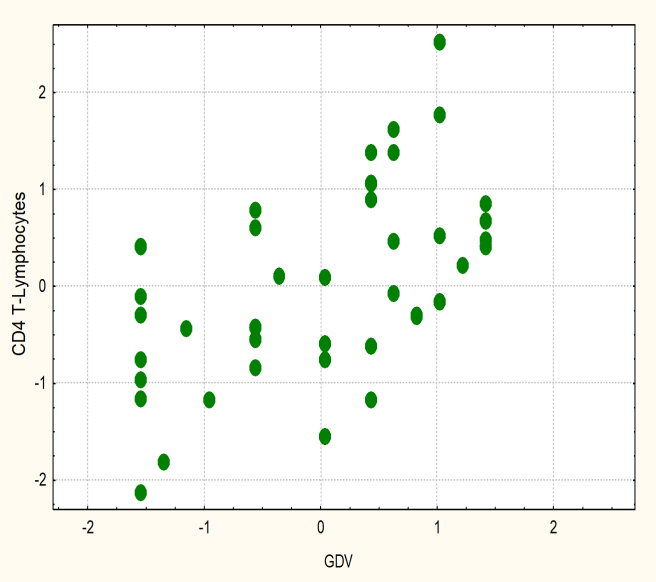

Fig. 3. Scatterplot of canonical correlation between GDV parameters (X-line) and $CD4^+CD3^+$Th-lymphocytes level (Y-line)

The level of T-lymphocytes with high affinity is subject to downregulation by the asymmetry of the fifth and fourth chakras, as well as the energy of the seventh chakra. The degree of determination is 25% (Table 3 and Fig. 4).

Table 3. Regression Summary for Dependent Variable: "active" T Lymphocytes
R=0,572; R^2=0,327; Adjusted R^2=0,250; $F_{(4,3)}$=4,3; $\chi^2_{(4)}$=14,3; p=0,007; SE: 3,7 %

		Beta	St. Err. of Beta	B	St. Err. of B	$t_{(35)}$	p-level
	r		Intercpt	30,65	,64	48,2	10^{-6}
Ch5 A	-0,37	-,255	,147	-5,15	2,95	-1,74	,090
Ch4 A f	-0,34	-,289	,140	-4,65	2,25	-2,07	,046
Ch4 A	-0,31	-,249	,147	-3,30	1,95	-1,69	,099
Ch7 E	-0,25	-,235	,141	-4,15	2,49	-1,67	,105

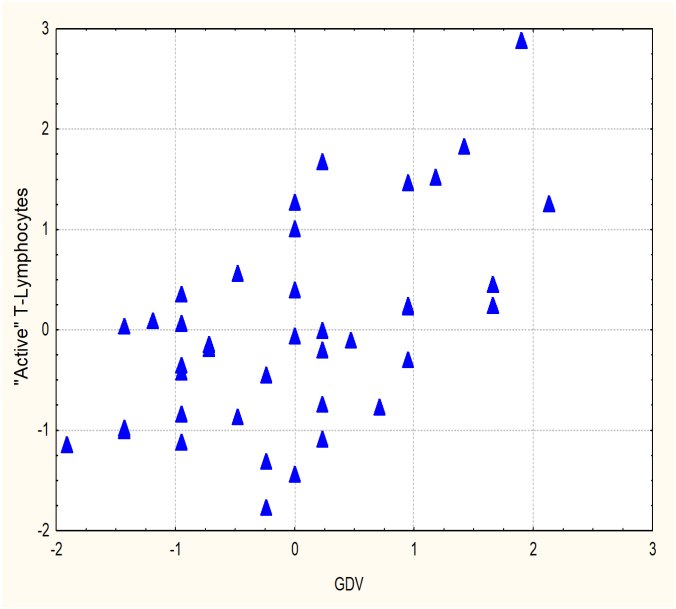

Fig. 4. Scatterplot of canonical correlation between GDV parameters (X-line) and "active" T-lymphocytes level (Y-line)

Downregulation of the third and sixth chakras of the level of natural killers is very weak (11%), but statistically significant (Table 4 and Fig. 5).

Table 4. Regression Summary for Dependent Variable: NK-Lymphocytes
R=0,396; R^2=0,156; Adjusted R^2=0,111; $F_{(2,4)}$=3,4; p=0,043; SE: 4,5 %

		Beta	St. Err. of Beta	B	St. Err. of B	$t_{(37)}$	p-level
	r		Intercpt	18,95	,85	22,39	10^{-6}
Ch3 A f	-0,28	-,307	,152	-6,19	3,06	-2,02	,050
Ch6 E	-0,25	-,280	,152	-4,58	2,49	-1,84	,073

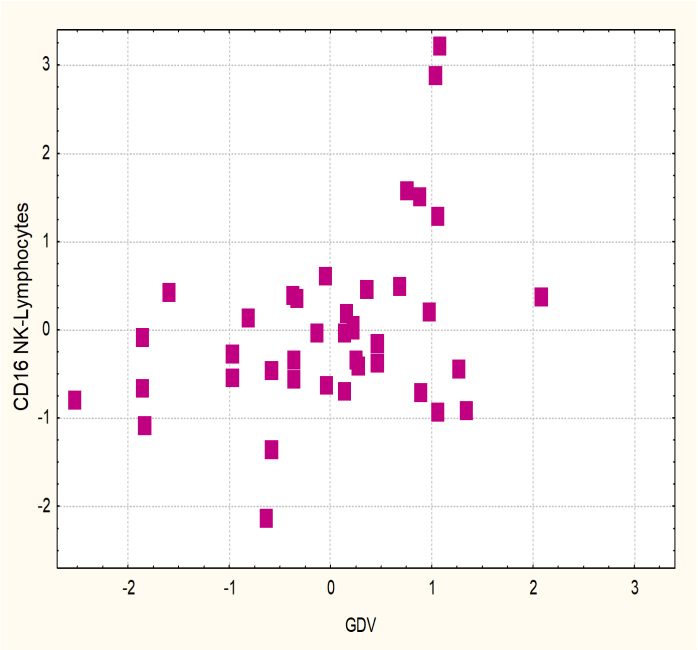

Fig. 5. Scatterplot of canonical correlation between GDV parameters (X-line) and NK-lymphocytes level (Y-line)

Instead, the relationship between B-lymphocyte levels and chakras is insignificant (Table 5 and Fig. 6).

Table 5. Regression Summary for Dependent Variable: $CD22^+$ B-lymphocytes
R=0,438; R^2=0,192; Adjusted R^2=0,099; $F_{(4,3)}$=2,1; $\chi^2_{(4)}$=7,7; p=0,105; SE: 4,0 %

		Beta	St. Err. of Beta	B	St. Err. of B	$t_{(35)}$	p-lev-el
	r		Intercpt	23,14	,66	35,0	10^{-6}
Ch4 A f	-0,21	-,301	,156	-4,84	2,52	-1,92	,063
Ch7 A	-0,16	-,270	,158	-3,93	2,29	-1,71	,096
Ch3 A	0,17	,284	,158	3,82	2,12	1,80	,080
Ch2 E	0,16	,227	,154	3,05	2,07	1,48	,149

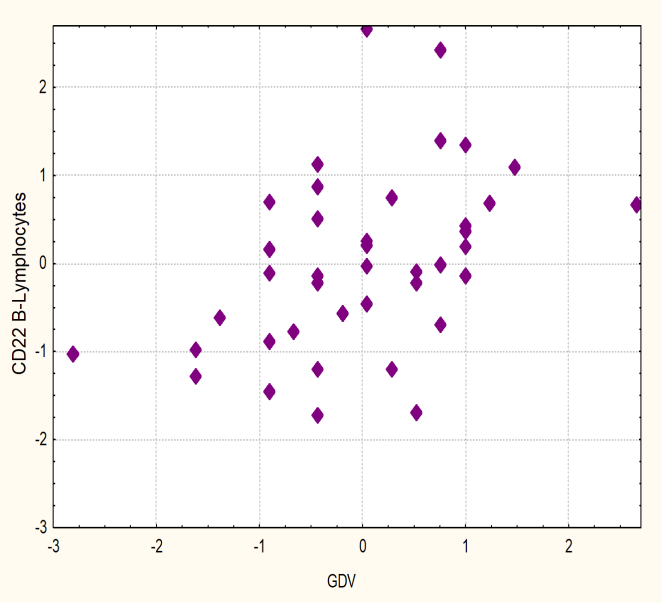

Fig. 6. Scatterplot of canonical correlation between GDV parameters (X-line) and CD22$^+$ B-lymphocytes level (Y-line)

The level of 0-lymphocytes calculated by the balance method (100-Tc-Th-B-NK) was associated with the symmetry of GDI and the energy of the sixth chakra, determined by these parameters by 14% (Table 6 and Fig. 7).

Table 6. Regression Summary for Dependent Variable: 0-Lymphocytes
R=0,457; R^2=0,209; Adjusted R^2=0,143; $F_{(3,4)}$=3,2; $\chi^2_{(3)}$=8,5; p=0,036; SE: 12,1 %

		Beta	St. Err. of Beta	B	St. Err. of B	$t_{(36)}$	p-level
	r		Intercpt	286,9	181,5	1,58	,123
Sym f	-0,34	-,202	,170	-2,52	2,11	-1,19	,240
Sym	-0,29	-,222	,169	-,59	,45	-1,32	,196
Ch6 E	0,28	,270	,151	12,14	6,81	1,78	,083

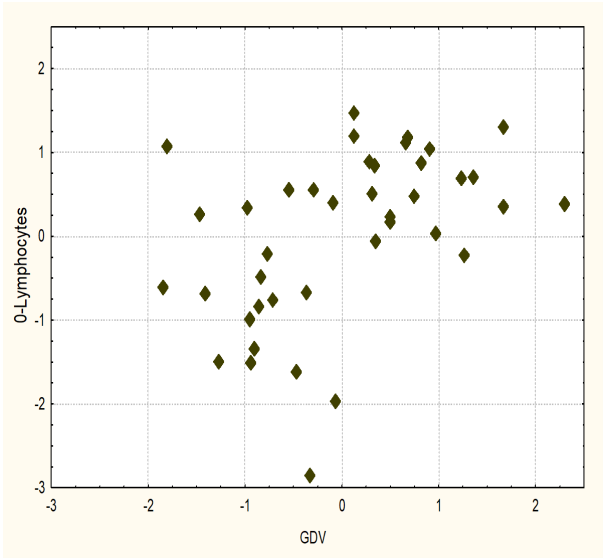

Fig. 7. Scatterplot of canonical correlation between GDV parameters (X-line) and 0-lymphocytes level (Y-line)

Immunocytogram entropy correlates with three GDV parameters at the significance limit (Table 7 and Fig. 8).

Table 7. Regression Summary for Dependent Variable: Entropy of Immunocytogram
R=0,429; R^2=0,184; Adjusted R^2=0,116; $F_{(3,4)}$=2,7; $\chi^2_{(3)}$=7,4; p=0,059; SE: 0,034

		Beta	St. Err. of Beta	B	St. Err. of B	$t_{(36)}$	p-level
	r		Intercpt	,162	,520	,31	,757
Sym f	0,30	,297	,154	,010	,005	1,93	,061
EL f	-0,26	-,175	,155	-,035	,031	-1,13	,268
Ch3 A f	-0,23	-,225	,155	-,034	,023	-1,45	,155

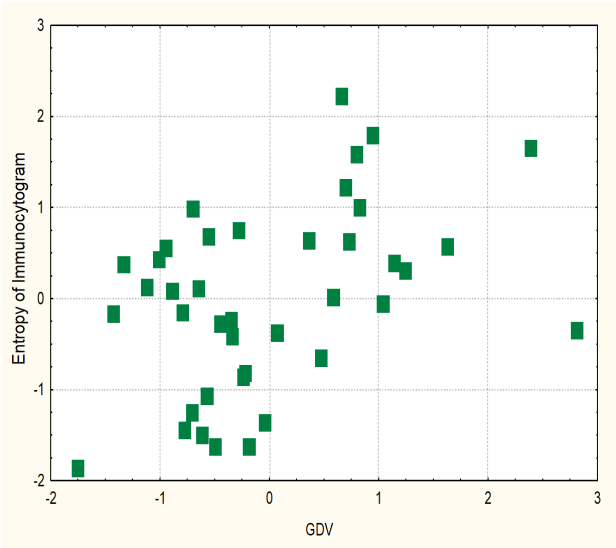

Fig. 8. Scatterplot of canonical correlation between GDV parameters (X-line) and Entropy of Immunocytogram (Y-line)

At the next stage, the analysis of the canonical correlation between the registered parameters of cellular immunity, on the one hand, and the parameters of GDV selected at the previous stage, on the other hand, was performed.

As a result, a pair of canonical roots were formed (Table 8). The program did not include B-lymphocytes in the structure of the immune root, apparently due to the insignificant coefficient of canonical correlation, but under the same conditions the entropy of the immunocytogram was still found in the factor structure of the root.

Table 8. Factor Structure of GDV and Cellular Immunity Canonical Roots

Left set	Root 1
Symmetry GDI f	**,64**
Ch7 Asymmetry f	**,35**
Symmetry GDI	**,33**
Ch6 Energy f	**-,50**
Ch6 Energy	**-,49**
Ch5 Energy	**-,40**
Ch4 Asymmetry	**-,32**
Ch4 Asymmetry f	**-,17**
Ch3 Asymmetry f	**-,15**
Ch5 Asymmetry	**-,15**
Entropy Left	**-,11**
Right set	Root 1
$CD4^+CD3^+$	**,86**
NK-Lymphocytes	**,59**
Entropy ICG	**,46**
$CD8^+CD3^+$	**,41**
T "active"	**,18**
0-Lymphocytes	**-,65**

The GDV-root represents 11 parameters, three of which give positive factor loads, which reflects their enhancing immunotropic effect, while the other 8 parameters have an immunosuppressive effect. Downregulation of 0-lymphocyte levels is physiologically favorable because it reflects the activation of receptor expression by immature immunocytes.

In general, the canonical correlation between the parameters of GDV and cellular immunity was strong, but it is unclear why statistically insignificant (Fig. 9).

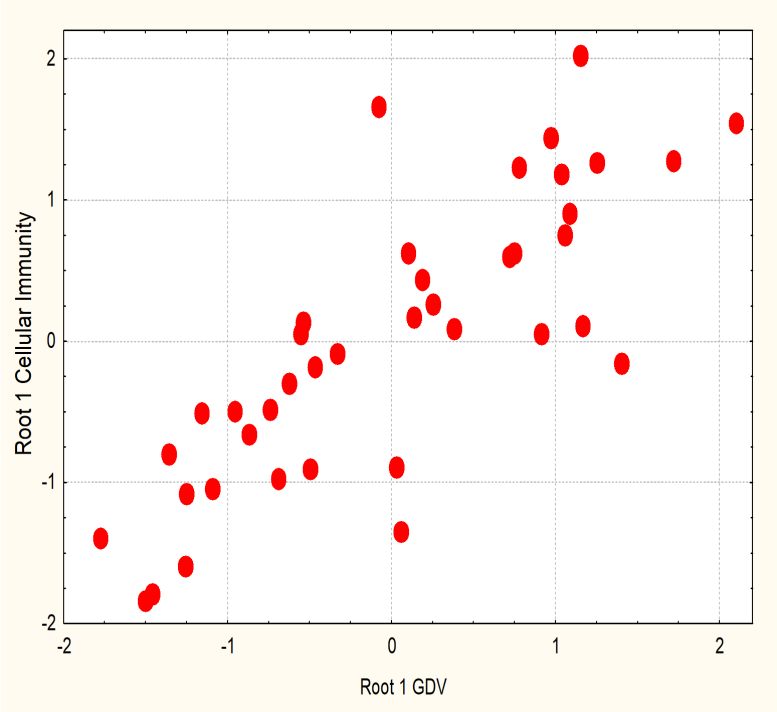

R=0,809; R^2=0,657; $\chi^2_{(84)}$=104; p=0,07; Λ Prime=0,026

Fig. 9. Scatterplot of canonical correlation between GDV parameters (X-line) and Cellular Immunity parameters (Y-line)

Among the parameters of humoral immunity, IgA was most closely related to the parameters of GDV. First of all, it is the energy of the fifth and sixth chakras (Fig. 10 and 11).

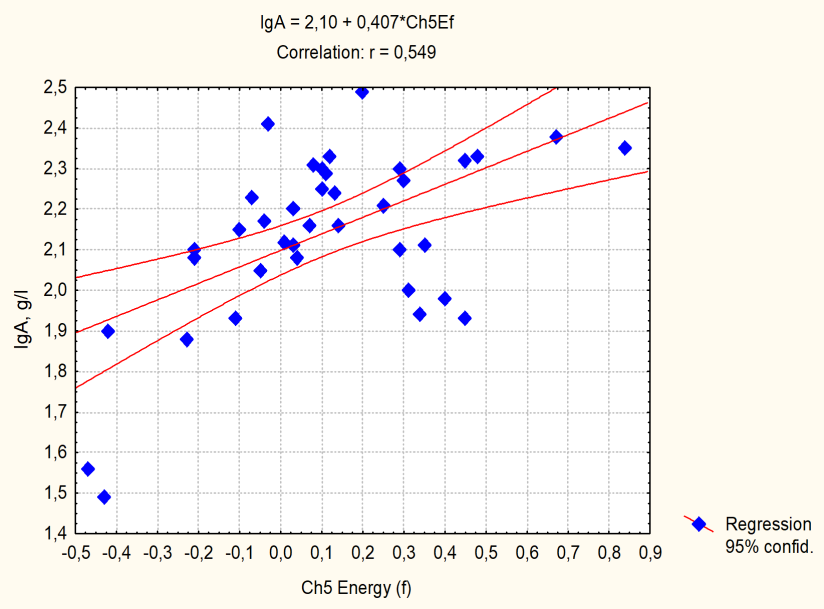

Fig. 10. Scatterplot of correlation between Chakra 5 Energy (f) (X-line) and IgA serum level (Y-line)

Significant influence on the level of IgA also have other parameters of GDV, in total determining it by 37% (Table 9 and Fig. 12).

Levels of Iggs of other classes are determined by the parameters of GDV less, in particular IgG by 33% (Table 10 and Fig. 13) and IgM by 35% (Fig. 14-15 and Table 11).

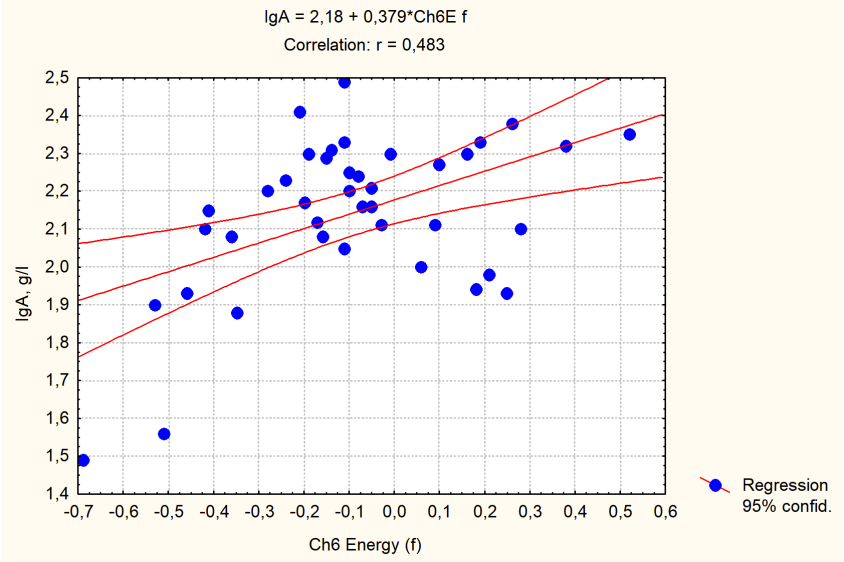

Fig. 11. Scatterplot of correlation between Chakra 6 Energy (f) (X-line) and IgA serum level (Y-line)

Table 9. Regression Summary for Dependent Variable: IgA
R=0,716; R^2=0,512; Adjusted R^2=0,366; $F_{(9,3)}$=3,5; $\chi^2_{(9)}$=24,0; p=0,005; SE: 0,16 g/L

		Beta	St. Err. of Beta	B	St. Err. of B	$t_{(30)}$	p-level
	r		Intercpt	1,890	1,319	1,43	,162
Ch6 E f	0,48	,526	,242	,413	,190	2,18	,038
Ch1 E f	0,44	,478	,332	,433	,301	1,44	,160
ER f	0,41	,463	,155	,623	,209	2,99	,006
Ch3 E f	0,34	-,384	,299	-,309	,241	-1,28	,210
Ch1 E	0,29	-,519	,264	-,343	,174	-1,97	,058
AL f	0,28	-,501	,296	-,00005	,00003	-1,69	,102
Ch7 E	0,27	,287	,208	,246	,178	1,38	,177
SL f	-0,27	-,319	,258	-,046	,037	-1,24	,226

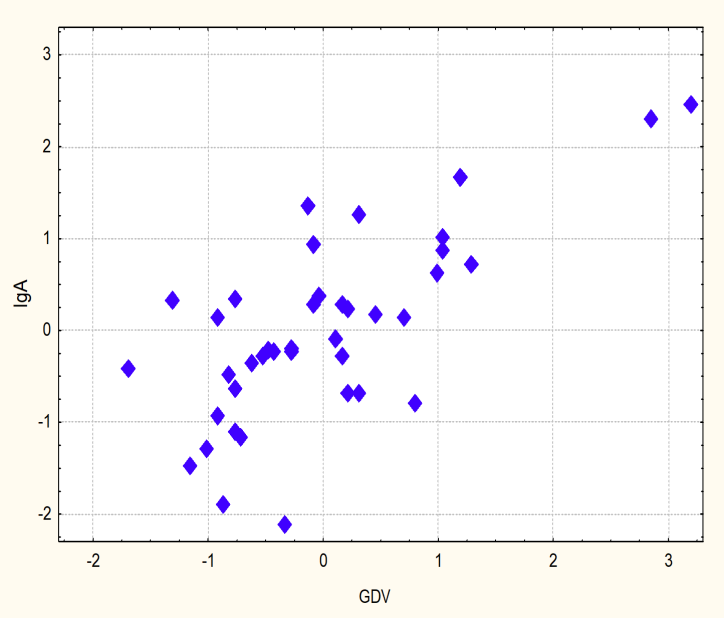

Fig. 12. Scatterplot of canonical correlation between GDV parameters (X-line) and IgA serum level (Y-line)

Table 10. Regression Summary for Dependent Variable: IgG
R=0,645; R^2=0,416; Adjusted R^2=0,331; $F_{(5,3)}$=4,9; $\chi^2_{(5)}$=19,1; p=0,002; SE: 2,7 g/L

		Beta	St. Err. of Beta	B	St. Err. of B	$t_{(34)}$	p-level
	r		Intercpt	8,93	5,29	1,69	,100
AF	0,40	,319	,220	,0003 1	,00021	1,45	,156
Ch7 E	0,35	1,005	,396	13,72	5,41	2,53	,016
Ch1 A	0,35	,313	,136	4,50	1,96	2,29	,028
Ch3 A	0,31	,320	,135	3,33	1,40	2,38	,023
Ch2 E	0,28	-,960	,434	-9,97	4,51	-2,21	,034

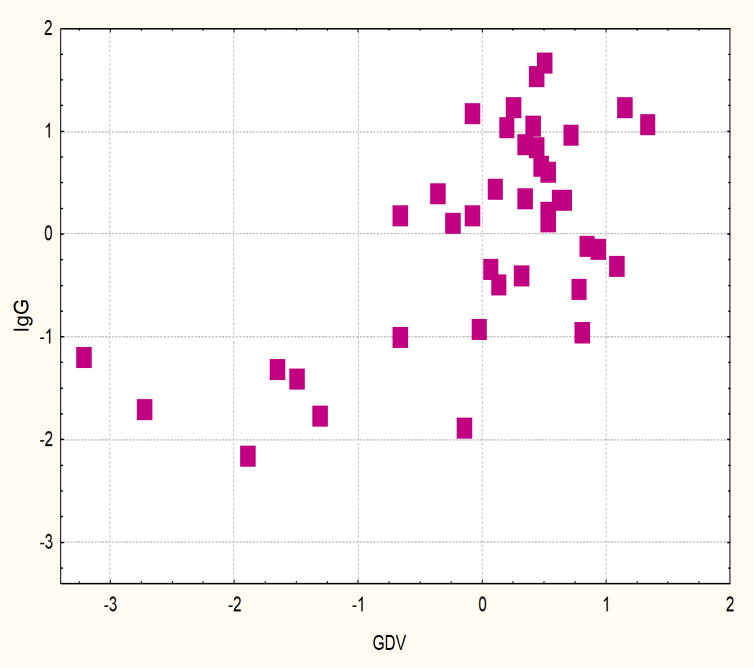

Fig. 13. Scatterplot of canonical correlation between GDV parameters (X-line) and IgG serum level (Y-line)

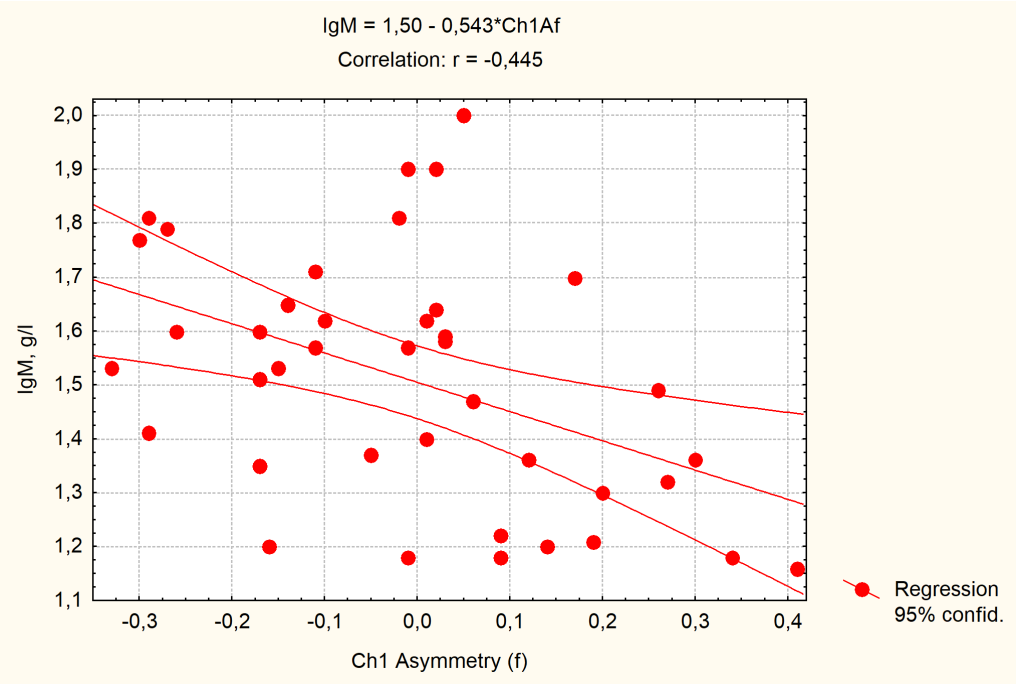

Fig. 14. Scatterplot of correlation between Chakra 1 Asymmetry (f) (X-line) and IgM serum level (Y-line)

Table 11. Regression Summary for Dependent Variable: IgM

R=0,622; R^2=0,387; Adjusted R^2=0,353; $F_{(2,4)}$=11,7; $\chi^2_{(2)}$=18,1; p=0,0001; SE: 0,18 g/L

		Beta	St. Err. of Beta	B	St. Err. of B	$t_{(37)}$	p-level
	r		Intercpt	1,511	,029	51,66	10^{-6}
Ch1 A f	-0,44	-,547	,132	-,668	,162	-4,13	,0002
Ch7 E f	-0,32	-,447	,132	-,546	,162	-3,38	,002

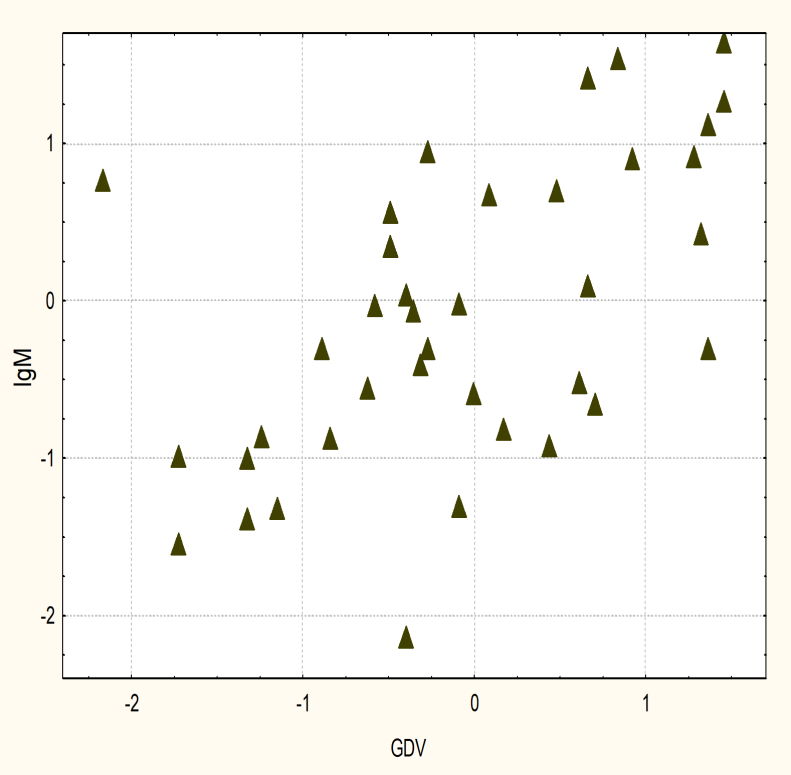

Fig. 15. Scatterplot of canonical correlation between GDV parameters (X-line) and IgM serum level (Y-line)

And the weakest were the links between the parameters of GDV and the level of circulating immune complexes (Table 12 and Fig. 16).

Table 12. Regression Summary for Dependent Variable: CIC
R=0,491; R^2=0,241; Adjusted R^2=0,178; $F_{(3,4)}$=3,8; $\chi^2_{(3)}$=10,1; p=0,018; SE: 12 units

		Beta	St. Err. of Beta	B	St. Err. of B	$t_{(36)}$	p-level
	r		Intercpt	148,9	46,7	3,19	,003
EF	-0,37	-,347	,146	-29,45	12,39	-2,38	,023
Ch6 A f	-0,31	-,187	,161	-8,68	7,51	-1,16	,255
Ch1 E	-0,28	-,192	,161	-8,24	6,89	-1,20	,240

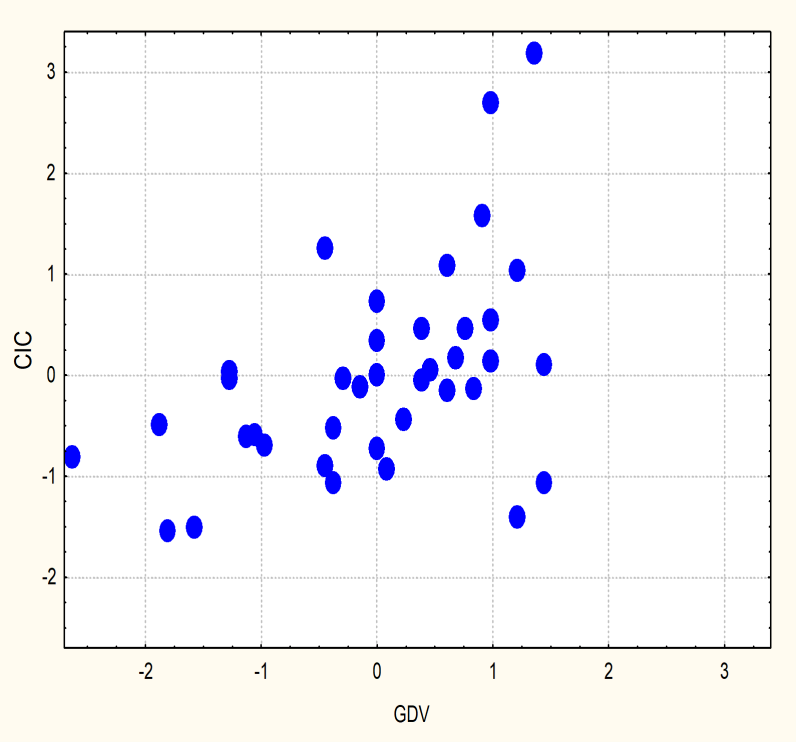

Fig. 16. Scatterplot of canonical correlation between GDV parameters (X-line) and CIC serum level (Y-line)

The result of the canonical correlation analysis shows that the determination of the GDV parameters of humoral immunity is much stronger than cellular: 81% vs 66% (Table 13 and Fig. 17).

Table 13. Factor Structure of GDV and Humoral Immunity Canonical Roots

Left set	Root 1
Ch1 Asymmetry	**,40**
Area Frontal	**,37**
Ch7 Energy	**,34**
Ch3 Asymmetry	**,34**
Ch2 Energy	**,25**
Area Left f	**,22**
Ch1 Energy f	**,19**
Ch5 Energy	**,18**
Ch2 Energy f	,08
Ch6 Energy f	,08
Ch7 Energy f	,06
Ch3 Energy f	,03
Entropy Frontal	**-,32**
Shape Left f	**-,15**
Ch6 Asymmetry f	**-,10**
Right set	Root 1
IgG	**,85**
IgM	**,57**
CIC	**,28**
IgA	**,24**

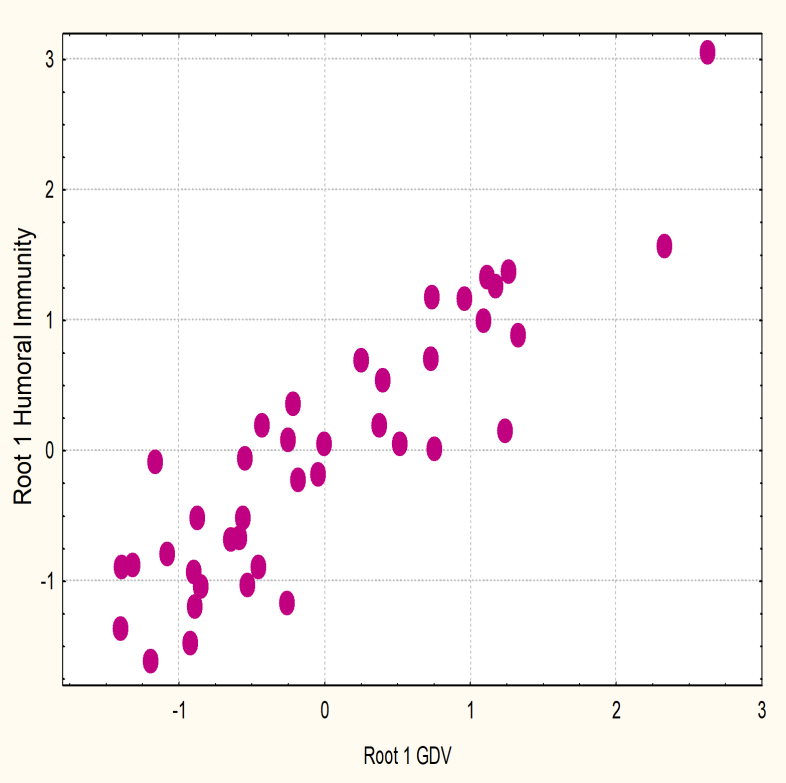

R=0,897; R^2=0,807; $\chi^2_{(68)}$=104; p=0,003; Λ Prime=0,024

Fig. 17. Scatterplot of canonical correlation between GDV parameters (X-line) and Humoral Immunity parameters (Y-line)

At the final stage, the analysis of the canonical correlation of cellular and humoral immunity parameters with GDV parameters was performed. As a preamble we set out the following provisions.

The GDV method is based on the registration of stimulated emission of photons and electrons from the skin surface. Korotkov KG [13,14] believes that GDV method measures the distribution of electron densities in human systems and organs. These electron densities are the main basis of physiological energy, so there is reason to say that the GDV method allows us to measure the body's potential energy reserve. GDI, taken off without filter, characterizes the functional changes of organism, while taken with a filter characterizes organic changes. At the same time, the GDV method is a bridge between the logical science of the West and the intuitive science of the East. It allows us to represent the same phenomena in different languages, in different systems, to look at the same things from different points of view.

According to Ayurvedic medicine, Chakras are power centers, related to the endocrine glands and neural plexus as well as to some organs. In Puchko LG [27] we read that the **first** Chakra is related to the testicles and sacral plexus, **second** Chakra to the ovaries, adrenals and kidneys, **third** Chakra to **spleen**, liver and solar plexus, **fourth** Chakra to **thymus**, heart and cardial plexus, **fifth** Chakra to thyroid and parathyroid glands, **sixth** Chakra to pituitary gland and brain, **seventh** Chakra to pineal gland. Chase CR [8] provides a table according to which the **first** Chakra is associated with adrenals, pelvic nerve plexus, spine, kidneys, bladder, large intestine; **second** Chakra with testes/ovaries, inferior mesenteric ganglion, ileum, organs of reproduction; **third** Chakra with [endocrine] pancreas, celiac plexus ganglion, liver, gall bladder, stomach, duodenum, pancreas, **spleen**; **fourth** Chakra with **thymus**, celiac plexus, heart, circulation, vagus nerve; **fifth** Chakra with thyroid and parathyroid glands, inferior cervical ganglion, lungs, bronchus, larynx, pharynx, large intestine, vagus nerve; **sixth** Chakra

with pituitary and pineal glands, thalamus, hypothalamus, superior cervical ganglion, left brain, lower brain, ears/nose, left eye; **seventh** Chakra with pineal gland, right brain, upper brain, right eye.

Korotkov KG [12] put forward the concept that each Chakra is associated with a part of the finger. This approach is embodied in the "GDV Chakras" program, which allows us to quantify the state of virtual Chakras.

According to the results of the canonical analysis, two pairs of roots are formed, which are almost identical in the coefficients R and R^2, but differ significantly in the factor structure (Table 14). Contrary to expectations, the parameters of the **fourth** and **third** Chakras, which are associated with the thymus and spleen, respectively, give only moderate factor loads, while the top positions are occupied by the parameters of the **seventh** and **second** Chakras. However, our shock quickly turns into antishock, given that these Chakras represent the pineal gland and brain and adrenals or sexual glands, respectively. The immunomodulatory effect of adrenal and gonadal hormones has long been known, as well as thyroid and parathyroid hormones [26,30,33] associated with the **fifth** Chakra, also present in the factor structure of the root. Now it became known about the immunomodulatory activity of the pineal gland [9,18,19,28]. Finally, one of the trends in modern neuroimmunology is the role of immunomodulation of the vagus [20,26,30-32] associated with the **fourth** and **fifth** Chakras, the activity of which, in turn, is controlled by the neural network [31,32]. The presence in the factor structure of the parameters of symmetry and asymmetry is perfectly consistent with the lateralization of cortical regulatory structures.

Table 14. Factor Structure of GDV and Immunity Canonical Roots

Left set	Root 1	Root 2
Ch7 Energy f	**-,48**	-,10
Ch2 Energy f	**-,46**	-,12
Ch7 Energy	**-,38**	,04
Ch2 Energy	**-,38**	-,05
Ch4 Asymmetry f	**-,31**	,23
Symmetry	**-,27**	-,22
Area Frontal	**-,26**	,17
Area Left f	**-,26**	,15
Ch5 Energy	**-,25**	,21
Ch4 Asymmetry	**-,23**	,21
Ch6 Energy f	**-,23**	,20
Ch3 Energy f	**-,21**	-,03
Ch1 Energy f	**-,20**	,01
Entropy Left f	**,28**	**,24**
Ch5 Asymmetry	**-,23**	**,24**
Ch6 Energy	**-,22**	**,25**
Ch1 Asymmetry	-,16	**,37**
Symmetry f	,10	**-,43**
Ch1 Asymmetry f	**-,30**	**-,34**
Right set	Root 1	Root 2
T "active"	**,60**	-,41
IgM	**,43**	,37
CIC	**,16**	,06
IgA	**-,33**	-,01
$CD4^+CD3^+$ Th	,07	**-,46**
$CD8^+CD3^+$ Tc	-,22	**-,40**
Entropy ICG	-,17	**-,36**
$CD16^+$ NK	-,11	**-,14**
0-Lymphocytes	,11	**,44**
IgG	-,21	**,37**

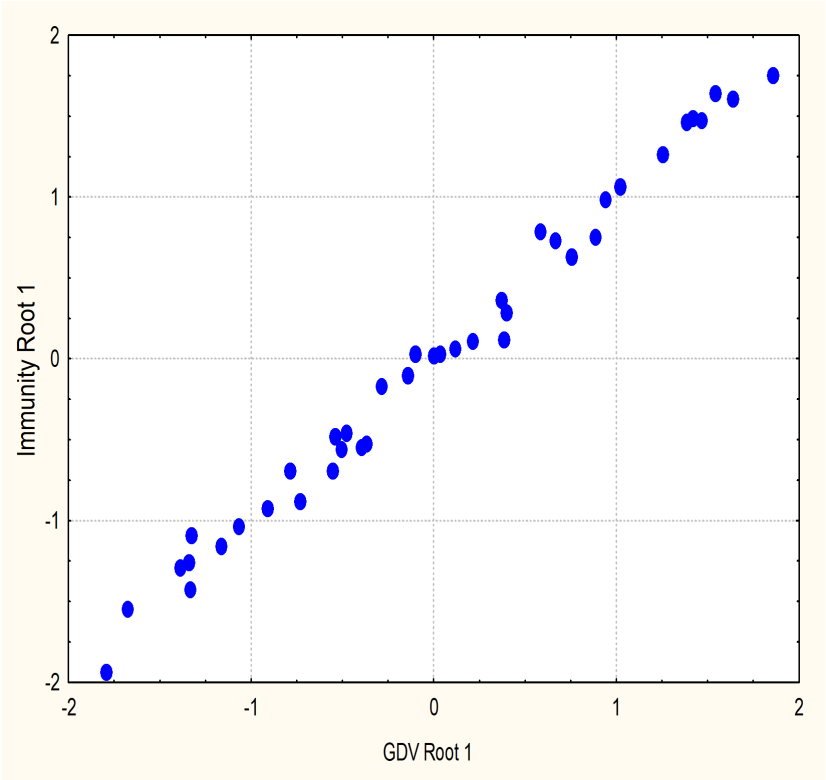

R=0,994; R^2=0,988; $\chi^2_{(280)}$=388; p<10^{-4}; Λ Prime<10^{-6}

Fig. 18. Scatterplot of canonical correlation between GDV parameters (X-line) and all Immunity parameters (Y-line). The first pair of roots

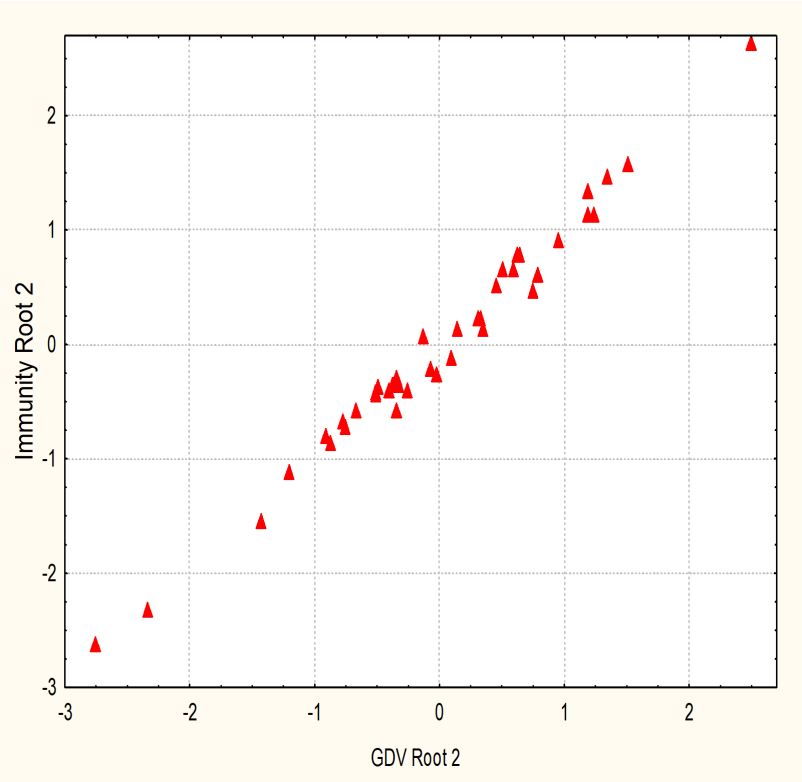

R=0,992; R^2=0,984; $\chi^2_{(243)}$=341; p=0,007; Λ Prime<10^{-6}

Fig. 19. Scatterplot of canonical correlation between GDV parameters (X-line) and all Immunity parameters (Y-line). The second pair of roots

Judging by the coefficients of determination (Fig. 18 and 19), the parameters of GDV almost totally regulate the state of immunity.

We secretly hope that we have convinced our colleagues, adherents of Western medicine, that the method of GDV is quite relevant, and the Chakras are not fiction but reality. Subsequent publications will present data on the relationship of GDV parameters with the electrical conductivity of acupuncture points and EEG and metabolism parameters.

ACKNOWLEDGMENT

We express sincere gratitude to administration JSC "Truskavets'kurort" for help in carrying out immune analyzes. Special thanks to the volunteers.

ACCORDANCE TO ETHICS STANDARDS

Tests in volunteers are conducted in accordance with positions of Helsinki Declaration 1975, revised and complemented in 2002, and directive of National Committee on ethics of scientific researches. During realization of tests from all participants the informed consent is got and used all measures for providing of anonymity of participants.

REFERENCES

1. Babelyuk VYe. The parameters of gas discharge visualization (kirlianogram) appropriately associated with some psychophysiological and endocrine parameters of healthy men. Medical Hydrology and Rehabilitation. 2013; 11(1): 21-30.

2. Babelyuk VYe, Dubkova GI, Korolyshyn TA, Zukow W, Popovych IL. The correlationships between parameters of gas discharge visualization and principal neuroendocrine factors of adaptation. In: Pathophysiology and Pharmacy: ways of integration. Abstracts VII National Congress of Pathophysiologists Ukraine with international participation (5-7 October 2016). Kharkiv. NPhU; 2016: 8-8.

3. Babelyuk VYe, Dubkowa GI, Korolyshyn TA, Holubinka SM, Dobrovolsky YG, Zukow W, Popovych IL. Operator of Kyokushin Karate via Kates increases synaptic efficacy in the rat Hippocampus, decreases C3-θ-rhythm SPD and HRV Vagal markers, increases virtual Chakras Energy in the healthy humans as well as luminosity of distilled water in vitro. Preliminary communication. Journal of Physical Education and Sport. 2017; 17(1): 383-393.

4. Babelyuk VE, Gozhenko AI, Dubkova GI, Babelyuk NV, Zukow W, Kovbasnyuk MM, Popovych IL. Causal relationships between the parameters of gas discharge visualization and principal neuroendocrine factors of adaptation. Journal of Physical Education and Sport. 2017; 17(2): 624-637.

5. Babelyuk VY, Dubkova HI, Korolyshyn TA, Mysula IR, Popovych DV, Popovych IL, Zukow W. Relationships between caused by Kozyavkin© method changes in parameters of manual function and electroencephalogram, heart rate variability as well as gas discharge visualization in children with spastic form of cerebral palsy. Journal of Education, Health and Sport. 2018; 8(4): 159-194.

6. Babelyuk VYe, Popadynets' OO, Dubkova GI, Zukow W, Muszkieta R, Gozhenko OA, Popovych IL. Entropy of gas-discharge image correlates with the entropies of EEG, immunocytogram and leukocytogram but not HRV. Pedagogy and Psychology of Sport. 2020; 6(2): 30-39.

7. Babelyuk VYe, Popovych IL, Babelyuk NV, Korolyshyn TA, Dubkova GI, Kovbasnyuk MM, Hubyts'kyi VYo, Kikhtan VV, Musiyenko VYu, Kyrylenko IG, Dobrovolsky YG, Korsuns'kyi IH, Muszkieta R, Zukow W, Gozhenko AI. Perspectives on the use of electrostimulation with the device "VEB"® in the management of disorders related to COVID-19. Balneo Research Journal. 2020; 11(3): 328-343.

8. Chase CR. The Geometry of Emotions: Using Chakra Acupuncture and 5-Phase Theory to Describe Personality Archetypes for Clinical Use. Med Acupunct. 2018; 30(4): 167-178.

9. Csaba G. The Immunoendocrine Thymus as a Pacemaker of Lifespan. Acta Microbiol Immunol Hung. 2016; 63(2): 139-158.

10. Gozhenko AI, Sydoruk NO, Babelyuk VYe, Dubkowa GI, Flyunt VR, Hubyts'kyi VYo, Zukow W, Barylyak LG, Popovych IL. Modulating effects of bioactive water Naftussya from layers Truskavets' and Pomyarky on some metabolic and biophysic parameters at humans with dysfunction of neuro-endocrine-immune complex. Journal of Education, Health and Sport. 2016; 6(12): 826-842.

11. Kindzer BM, Babelyuk VY, Babelyuk NV, Popovych IL, Dubkova GI, Dobrovolsky YG, Korsuns'kyi IH, Korolyshyn TA, Litosh S, Kindzer H, Zukow W. The device for electrostimulation "VEB-1" modulates parameters of electroencephalogram and gas discharge visualization. Science and society. Proc. of the 11th internat. confer. Acent Grafics Communications and Publishing. Hamilton, Canada. 2019: 159-171.

12. Korotkov KG. Basics GDV Bioelectrography [in Russian]. SPb. SPbGITMO(TU); 2001: 360 p.

13. Korotkov KG. Principles of Analysis in GDV Bioelectrography [in Russian]. SPb. Renome; 2007: 286 p.

14. Korotkov KG. Energy Fields Electrophotonic Analysis in Humans and Nature. Second updated edition. Translated from Russian by the author. Edoted by Berney Williams and Lutz Rabe. 2014: 233 p.

15. Kozyavkina OV, Kozyavkina NV, Voloshyn TB, Hordiyevych MS, Lysovych VI, Babelyuk VY, Dubkova HI, Korolyshyn TA, Mysula IR, Popovych DV, Zukow W, Popovych IL. Caused by Kozyavkin© method changes in hand function parameters in children with spastic form of cerebral palsy and their EEGs, HRVs and GDVs accompaniments. Journal of Education, Health and Sport. 2018; 8(10): 11-30.

16. Kozyavkina OV, Kozyavkina NV, Hordiyevych MS, Voloshyn TB, Lysovych VI, Babelyuk VY, Dubkova HI, Korolyshyn TA, Popovych DV, Mysula IR, Zukow W, Popovych IL. Forecasting caused by Kozyavkin© method changes in hand function parameters in children with spastic form of cerebral palsy at their baseline levels as well as EEGs, HRVs and GDVs. Achivements of Clinical and Experimental Medicine. 2018; 4: 17-35.

17. Lapovets' LYe, Lutsyk BD. Laboratory Immunology [in Ukrainian]. Kyïv. 2004: 173 p.

18. Markus RP, Ferreira ZS, Fernandes PA, Cecon E. The immune-pineal axis: a shuttle between endocrine and paracrine melatonin sources. Neuroimmunomodulation. 2007; 14(3-4): 126-133.

19. Markus RP, Fernandes PA, Kinker GS, da Silveira Cruz-Machado S, Marçola M. Immune-pineal axis - acute inflammatory responses coordinate melatonin synthesis by pinealocytes and phagocytes. Br J Pharmacol. 2018; 175(16): 3239-3250.

20. Marques-Deak A, Cizza G, Sternberg E. Brain-immune interactions and disease susceptibility. Mol Psychiatry. 2005; 10(3): 239-250.

21. Muehsam D, Chevalier G, Barsotti T, Gurfein BT. An Overview of Biofield Devices. Glob Adv Health Med. 2015; 4(Suppl): 42-51.

22. Popadynets' OO, Gozhenko AI, Zukow W, Popovych IL. Relationships between the entropies of EEG, HRV, immunocytogram and leukocytogram. Journal of Education, Health and Sport. 2019; 9(5): 651-666.

23. Popovych IL, Babelyuk VYe, Dubkova GI. Relations between the parameters bioelectrography (kirlianography) and heart rate variability and blood pressure [in Ukrainian]. Medical Hydrology and Rehabilitation. 2010; 8(1): 4-16.

24. Popovych IL, Babelyuk VY, Dubkova HI, Korolyshyn TA, Zukow W. Relationships between changes in parameters of manual function and electroencephalogram, heart rate variability as well as gas discharge visualization in children with spastic form of cerebral palsy caused by Kozyavkin© method. Experimental and Clinical Physiology and Biochemistry. 2018; 1(81): 39-50.

25. Popovych IL, Babelyuk VYe, Zukow W, Muszkieta R, Dubkova GI, Nesterova LF, Hubyts'kyi VY, Bilas VR, Musienko VY, Seniv TS, Mis'ko VT, Babylyuk RV, Yaremchuk YM, Barylyak LG, Zukow W, Gozhenko AI. Liturgy affects the parameters of gas discharge visualization, acupuncture points and neuro-endocrine-immune complex. Pedagogy and Psychology of Sport. 2020; 6(2): 61-73.

26. Popovych IL, Gozhenko AI, Zukow W, Polovynko IS. Variety of Immune Responses to Chronic Stress and their Neuro-Endocrine Accompaniment. Scholars' Press. Riga; 2020: 172 p.

27. Puchko LG. Multidimensional Medicine. Systen of Self-diagnosis and Self-healing of Human [in Russian]. 10th ed., rev. and ext. Moskva: ANS, 2004. 432 p.

28. Rezzani R, Franco C, Hardeland R, Rodella LF. Thymus-Pineal Gland Axis: Revisiting Its

Role in Human Life and Ageing. Int J Mol Sci. 2020; 21(22): 8806.

29. Shannon CE. Works on the theory of informatics and cybernetics [transl. from English to Russian]. Moskva. Inostrannaya literatura; 1963: 329 p.

30. Sternberg EM. Neural regulation of innate immunity: a coordinated nonspecific host response to pathogens. Nat Rev Immunol. 2006; 6(4): 318-328.

31. Thayer JF, Sternberg EM. Neural aspects of immunomodulation: Focus on the vagus nerve. Brain Behav Immun. 2010; 24(8): 1223-1228.

32. Tracey KJ. Reflex control of immunity. Nat Rev Immunol. 2009; 9(6): 418-428.

33. Uchakin PN, Uchakina ON, Tobin BV, Ershov FI. Neuroendocrine immunomodulation [in Russian]. Vestnik Ross AMN. 2007; 9: 26-32.